An Innovative Approach to Evaluating Protection Level of Tight-Fitting PAPRs when Face Seal Is Compromised

Dmitri Kazakov[1*], Graham Powe[1], and Jintuo Zhu[2]

[1] Safety Equipment Australia Pty Ltd, Private Bag 1001, Mona Vale, NSW, 1660, AUSTRALIA
[2] School of Safety Engineering, China University of Mining and Technology, Xuzhou, Jiangsu, CHINA

* Corresponding author and E-mail: Dmitri.Kazakov@sea.com.au

ABSTRACT

Few studies have been done to investigate the ability of tight-fitting Powered Air Purifying Respirators (PAPRs) to compensate for face seal leaks, and this project developed an innovative approach to evaluating the protection level of PAPRs when the face seal is compromised. For this study, a cross sectional area of seal leaks versus a reduction in protection factor was used to evaluate the potential effect of a simulated leak on PAPRs during over breathing whilst exercising on a bicycle.

It was found that the ability of PAPRs to maintain positive pressure cannot be assessed by constant-flow measurement or by the sinusoidal profile of a breathing machine, however it can be assessed by collecting pressure data from inside the mask during TIL human exercise and analysing the cumulative "weight" of the negative-pressure events. Furthermore, the pressure fluctuation representing Work of Breathing does not show as much variation as the variation of the mask leakage, and some PAPRs have even larger pressure variation in comparison to the negative-pressure masks. It was concluded that the PAPRs tested are not so much breathing-assisting respirators as they are mask-leak compensation devices. PAPRs can provide additional face seal protection to the wearer in the event of mask leakage. Some PAPRs significantly outperformed the Air Purifying Respirators (APRs) (by 1900 times) whilst others minimally exceeded the protection of APRs (by 2 times) with a greater pressure variation (caused by the breathing resistance due to motor/impeller inertia) during the breathing cycles at high workloads.

Keywords: PAPR, APR, Powered Air Purifying Respirators, PAPR test, over breathing, flow, face seal, face fit, mask seal, protection factor, inhalation, exhalation, mask pressure, breathing resistance, Work of Breathing, positive pressure, motor, impeller, breathing machine, TIL test

Introduction

During the COVID pandemic, a large variety of new masks appeared on the market. N95 filtration level protection, for example, is not only advocated by government agencies, but extensively used as a major marketing tool by many resellers and manufacturers. But is such respirator approval, that emphasizes filtration performance and does not assess the quality of fit, more important compared to other factors such as mask style and other performance characteristic of the filtration medium?

Testing protection performance for tight-fitting powered air purifying respirators (PAPRs) is usually limited to measuring the operational airflow the PAPR can deliver, along with a total inward leakage (TIL) test when the wearer carefully adjusts the respirator to pass the fit test, such as in (Australian/New Zealand

Standard AS/NZS, 1716:2012). In the recent development of certification standards, attention has been paid to the Work of Breathing (WoB) (ISO/TS 16976-4:2019, Respiratory protective devices). It is well-known that the facial seal of even a perfectly fitted respirator may be broken during use. However, few studies have been done to investigate the ability of tight-fitting PAPRs to compensate for face seal leaks. Therefore, this study evaluates a PAPR's ability to compensate for respirator leaks and underlines the importance of evaluating this function. The study was based on simulating different face fits for half-face respirators and tight-fitting PAPRs, which would provide a sense of how critical the face seal is in respect to the protection performance. Based on this knowledge we can then evaluate the ability of different brands of PAPRs to compensate for leaks. This study is presented in two sections: 1) Effect of the physical size of the face seal leakage on the mask's protection factor, by simulating different sized leak orifices and correlating them with the protection performance for negative pressure respirators. 2) Comparison of different PAPRs' ability to compensate for face seal leakage during real work by calculating potential leak flow for different brands of tight-fitting PAPRs based on negative-pressure events.

This research was conducted in 4 consecutive stages. Firstly, this study quantified the variations of the protection factor of N95 respirators depending on how it is fitted to the headform, where the protection factor was calculated as follows:

$$Protection\ factor = \frac{Particle\ concentration\ inside\ the\ chamber}{Particle\ concentration\ inside\ the\ respirator}$$

$$Efficiency = \frac{1}{Protection\ factor} * 100\%$$

In the second stage of the experiment, we tested the effectiveness of respirators when introducing different size holes. Controlled leaks were introduced to the respirator by means of a set of calibrated orifices of various aperture sizes, and the influence of these leaks on the inhaled air quality was investigated. When we introduced a face seal leak of calibrated orifices into the filtration media of a very high (close to 100%) efficiency respirator, we observed how an increase in the orifice diameter reduces the level of protection. This test shows that the size of a hole in the media relates to the level of protection of a respirator, and demonstrates that eliminating all possible leaks around the face (i.e. correctly fitting the mask) can be more important than the choice of a mask/respirator itself. The different sizes of orifices were characterised by applying different pressures and by measuring the flow through the orifice.

In the third stage, a pressure logging device was used to create a profile of the pressure inside a tight-fitting respirator, and to convert the pressure to the leakage rate through calibrated orifices. Thereafter, we recalculate the volume of the leakage of contaminated air passing through the orifice to the internal zone of the respirator. We verified this testing method by running the setup on a breathing machine with a sinusoidal profile and a known breathing rate and volume. Knowing the total breathing volume (defined by the breathing machine) and the leak volume through the calibrated orifice, we calculated the protection factor of the respirator with the leak. Accordingly, we verified our method by comparing calculated and measured protection factors.

In the fourth section of this project, we applied the same method described above to calculate the protection factor of different brands of PAPRs worn by human subjects. This test was conducted whilst exercising on a bicycle programmed to increase the load gradually as well as including speech events. This test exposed the ability of various PAPRs to provide protection by positive pressure in response to the same facial leak. At the same time, we also analysed the PAPRs ability to compensate for the pressure variation inside the mask (due to the inhalation/exhalation cycle), which represents the breathing resistance for the PAPR user.

Based on these findings, further research and testing should be considered and introduced into Standard testing for PAPRs.

Preliminary Study of the Contribution of Leakage Sources to Filtering Facepiece Protection Performance

Equipment for Measurement of Protection Factor

- SEA Particle test chamber (Figure 1)
- Breathing machine Spirotest 2000 with Sheffield dummy hard face head fitted (Figure 2)
- Photometer DustTrack TSI8533 (Figure 3)
- Polydisperse particle generator Atomizer TSI3076 running challenge component Emery3004, average particle size 0.3 µm; Pressure generator Sundström SR79 running at 2.4 bar (Figure 4)
- A modified SR100 (Sundström) half-face elastomeric respirator: glued to the base with fitting to the Sheffield dummy head without any leak (Figure 8).

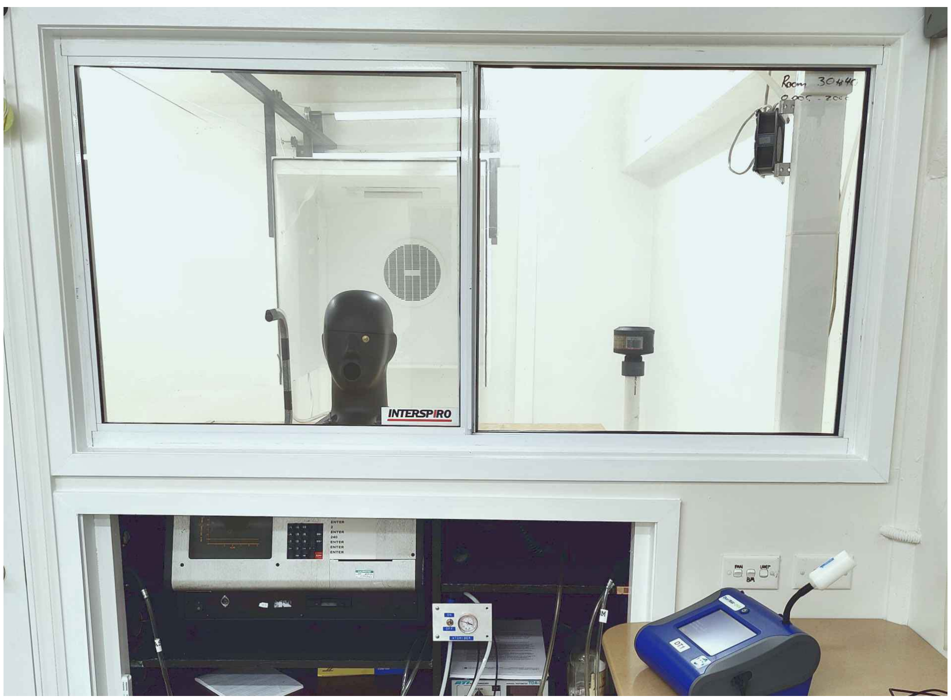

Figure 1: SEA Test chamber with the test head connected to the Breathing machine (below).

Figure 2: Breathing machine to simulate human breathing.

Figure 3: Photometer to test particle concentration.

Figure 4: Pressure/flow source and atomizer to generate the particles.

Air sampling probes were installed in the environmental chamber and in the volume inside the mouth of the headform. These were connected to the photometer for sampling ambient particle concentration and concentration inside the mask in the mouth area to evaluate the level of protection. All measuring instruments were calibrated according to NATA (National Association of Testing Authorities) standards before experiments.

Test Procedure

For each determination of protection factor, a respirator was fitted to the headform. The breathing machine was operated with a sinusoidal breathing pattern at 2 L minute volume and rate of 25 breaths per minute (BPM) rate, and air sampling conducted until the photometer reading was stabilized. Then the respirator was re-fitted with sealing to eliminate all fit imperfection and the protection factor measured again. The difference shows the contribution of the face seal leakage to the overall protection. To achieve better understanding the exact source of leaks, the respirator's edges were pressed to the headform by operator in different places and the particle concentration inside the mask was monitored.

In summary, as presented in Figure 5, the following tests were performed:

- The respirator was carefully fitted to the face and held by the straps;
- The respirator also pressed to the face on perimeter by hand to reduce potential for leakage;
- The respirator was glued to a test jig which is attached to the headform to eliminate face leaks so only the performance of filtration medium is tested;

Figure 5: Test configurations of one negative-pressure P2 filtering facepiece respirator with ear loops (PPETECH).

Results

The results are presented in Table I. Leakage and the consequent measured protection factor arise from a combination of filtration medium imperfection, face-seal leakage and, where present, exhalation valve leakage. Particle concentrations were measured with a resolution of 0.001 mg/m^3.

Pressing the respirator edges to the headform yielded a significant reduction in leakage; the protection factor improved more than 6 times. The last test configuration for which all the air passed only through the filtration medium improved the protection to 9 times the original fitting. The test showed that the quality of fitting was extremity important and an incorrectly fitted respirator can completely eliminate the effect of a good medium.

Table I. Fitting Effect on P2 Negative-Pressure Respirator on the Overall Protection

Test conditions	Chamber concentration, mg/m^3	Mask concentration, mg/m^3	Leak	Protection factor
Fitted with straps	30.2	19	62.9%	1.6
Sealed with hands	29.8	2.87	9.6%	10.4
Glued	27.6	1.8	6.5%	15.3

Similar tests were performed with another filtering facepiece respirator (3M model 9322A, See Figure 6). The respirator was known, from prior testing, to outperform many other types because of the better medium and facial seal. The results are presented in Table II.

Figure 6: 3M filtering facepiece respirator mounted on the headform (left) and edges of the respirator forced to the face to improve the face seal (right).

Table II. Quality of Fitting Effect on 3M respirator Overall Protection

Test conditions	Chamber concentration, mg/m^3	Mask concentration, mg/m^3	Leak	Protection factor
Fitted with straps	31.8	1.29	4.1%	24.6
With hands	31.8	0.39	1.2%	81.5
Glued	28.1	0.47	1.7%	59.8

The result was unexpected as better protection is achieved by compressing the respirator to the headform with the hand around the seal area, and further investigation showed that the foam at the nose area inside the mask (see the arrow on Figure 7) is an open cell foam that contributes to the leak. When the foam was compressed by the hand again, the mask leakage was reduced, and the protection factor increased.

Figure 7: 3M respirator is glued to the test plate. The arrow points to the foam on the nose bridge.

These results show that the respirator face seal plays a significant role in protection. Even a minor gap between the mask could be more critical than the quality of the filtration medium. The highest quality filtering facepiece with protection from the medium only (ideally the fitted mask with no leak) was 98.8% (protection factor 81.5). However, when we fit this respirator to the face with the straps, the protection factor reduced to 24.6 because of the face seal leaks. The protection can be significantly improved by fitting the mask to the face properly and by initial design considerations.

Face seal leak orifices and their characterization for elastomeric half-masks

Methods

The next series of tests was designed to quantify facepiece leakage by introducing an opening of known dimension. The test was performed in the test chamber with the respirator fitted to a headform connected to the breathing machine. The breathing machine was operated with a sinusoidal waveform with 2 L tidal volume and 25 BPM breathing frequency. To eliminate any sealing imperfection, the Sundstrom SR100 mask with an AS/NZS 1716-2012 P3 filter, modified with an orifice to create a leak, was fully sealed onto a plate (see Figure 8) and then connected to the breathing machine. Before the test, the system was tested to confirm there were no detectable leaks: with the chamber concentration of 34.1 mg/m^3, the photometer reading inside the mask was 0.000 mg/m^3 (see Figure 15). Taking into consideration the potential error caused by least significant digit of the display, we may assume that the concentration inside the respirator was lower than 0.001 mg/m^3, correspondingly, the initial protection factor of the fully sealed respirator including the filter was greater than 34,000 (or filtration efficiency > 99.997%). This is important for this test as we are operating the equipment close to the detection limit.

Figure 8: Modified Sundström mask SR100 and Filter SR510 with orifice fitted.

Figure 9: A set of calibrated orifices was used to simulate controlled breakage of face seal (0.15-4 mm).

A number of orifices with calibrated sizes of opening (Figure 9) were individually installed to the air boundary of the respirator (back plate, see Figure 8 right) to simulate different levels of faceseal leakage due to wear imperfections. The concentration was measured inside the chamber and then inside the facepiece for different orifices. After each measurement, time was given for the system to flush the particles and for the reading to stabilize. Leak flow rates can be calculated from the pressure differential across these orifices.

Calibration

The method to characterize the flow versus pressure across these orifices due to a very small airflow leakage was as follows: a Collins Spirometer was used to measure the volume of air under a bell submerged in water (see Figure 10). Changing the air volume under the bell caused the bell's position to displace vertically. The bell weight was compensated for by an external counterweight, so no noticeable pressure is required to keep the bell afloat. It requires minimal pressure to change the volume of the air under the bell. By applying additional weight to the bell or to the counterweight it is possible to create the pressure or vacuum under the bell, which will be constant and independent of the bell displacement due to the changing air volume under the bell. If we introduce the orifice into the pneumatic arrangement, the volume under the bell would change due to the leak through the orifice, while the applied pressure remains constant. Therefore, by timing the bell displacement, it is possible to calculate accurately the flow rate for any measured pressure. The orifices can be accurately characterized by determining leakage rates as the applied weight is changed.

Figure 10: Calibration setup.

During the test, the pressure was constantly monitored by a calibrated Valydine pressure transducer (Full Scale=14 cm H_2O, resolution 0.01 cm H_2O). This also confirmed that the pressure was constant for any bell position. The results are shown in Table III.

Table III. The results of Leak Flow vs Orifice Area

Orifice diameter mm	Calculated Orifice area, mm^2	Calculated Leak, mL/min			
		Pressure, cm H_2O =0	Pressure, cm H_2O =-0.66	Pressure, cm H_2O =-3.18	Pressure, cm H_2O =-8.27
0	**0**	0	0.00	0.00	0.00
0.15	**0.018**	0	5.58	21.52	35.03
0.35	**0.096**	0	31.9	82.8	144.2
0.5	**0.196**	0	59.6	153.8	265
0.7	**0.385**	0	129.1	307	52
1	**0.785**	0	284.3	694	1,135
1.4	**1.539**	0	588	1,324	2,270
2	**3.142**	0	1,367	2,830	5,298
2.8	**6.158**	0	2,943	6,030	/
4	**12.566**	0	6,232	9,856	/

The relation of leak flow vs orifice area is expected to be linear while all other parameters are held constant as shown in Figure 11. The little non-linearity of the leakage for the orifice (2.8 mm) at 3 cm H_2O pressure we believe is caused by air turbulence as during the test the orifice was noticeably “whistling”.

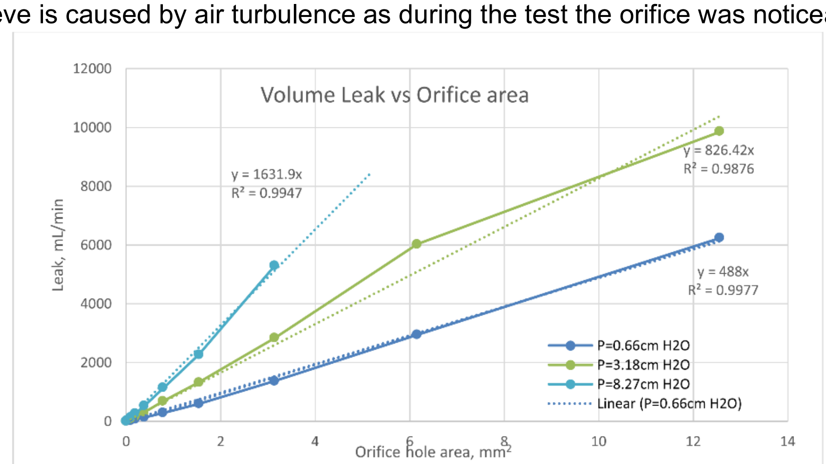

Figure 11: Leaks through the orifices expected to be linear with respect to opening area.

The pressure vs flow relationships are presented in Figure 12 and Figure 13.

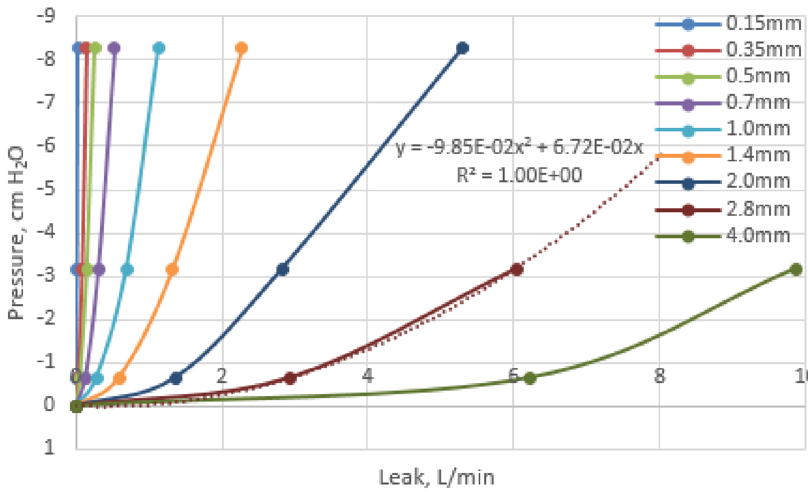

Figure 12: Pressure vs leak flow for all orifices.

The relationship can be described by parabolic equation $P = aF^2 + bF$, where *P* is pressure, *F* is leak flow. For orifice 2.8 mm the coefficients are a=-9.85E-02 and b=6.72E-02.

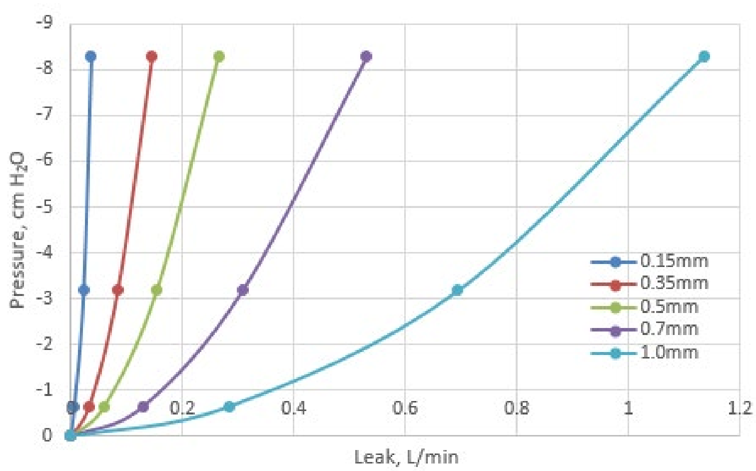

Figure 13: Pressure vs leak flow for orifices up to 1 mm diameter only.

Using these relationships, we can convert the pressure profile inside the respirator to the volume of the contaminated air entering through leak paths. By knowing the flow/pressure characteristics of the orifices, an appropriate orifice can be selected to represent a target leak rate through the equivalent hole in the ideal mask medium. For example, by this method, it could be determined that a previously tested respirator (see Table II, "Fitted with straps") with a protection level of 95.9% of ideal (including the face seal) was represented by a 2.5 mm diameter hole in the ideal medium. The respirator medium alone (excluding the face seal) has a protection level of 98.8% of ideal, which is equivalent to the leak through a 1.3 mm hole in diameter in the ideal medium.

Results

The results in Table IV and Figure 14 show that the fitting imperfection that is equivalent to an aperture size of 2.8 mm in diameter reduces the protection level to below 95% if ideal. These results are precise for this particular setup, however indicative in general because of the differences in the filter and respirator resistance. If the inhalation resistance of the respirator is higher, the inhalation pressure inside the mask is greater and the leak from the given orifice is larger.

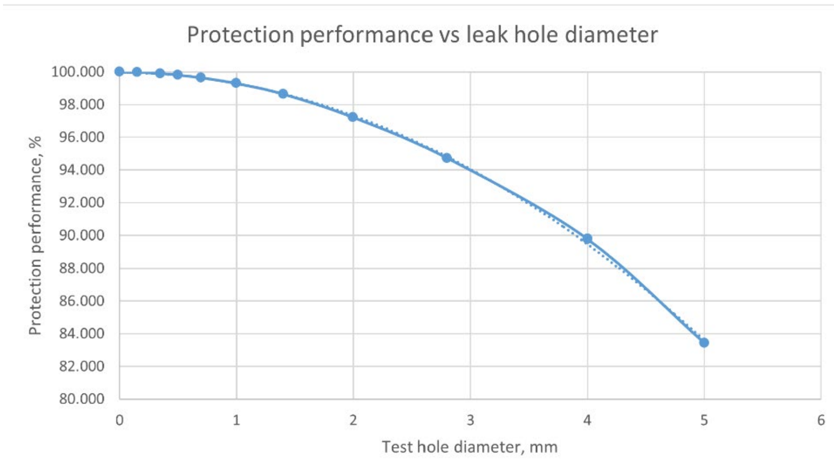

Figure 14: Graph representing the reduction in protection depending on the orifice diameter.

Table IV. Protection Factor vs Diameter of Orifice Aperture. Practical Test.

Orifice diameter	Challenge concentration	Resp. concentration	Protection factor	Resp. efficiency calculated
mm	mg/m³	mg/m³	/	%
0	34.1	0	>34100	99.997
0.15	32.7	0.008	4087.5	99.976
0.35	32.8	0.03	1093.3	99.909
0.5	34.1	0.065	524.6	99.809
0.7	36.2	0.129	280.6	99.644
1	31.1	0.22	141.4	99.293
1.4	31.7	0.43	73.7	98.644
2	34.5	0.96	35.9	97.217
2.8	36.6	1.93	19.0	94.727
4	32.7	3.34	9.8	89.786
5	32	5.3	6.0	83.438

Theoretical Calculation and Results Verification

During the test, the pressure and flow inside the respirator are captured by the SE-RDA unit as shown in Figure 15. The SE-RDA samples the pressure inside the respirator continuously at a sample rate of 50 samples per second.

Figure 15: Pressure and flow are logged by SE-RDA logger during the test. Concentration inside the chamber is 34.1 mg/m^3, inside the respirator is 0.000 mg/m^3.

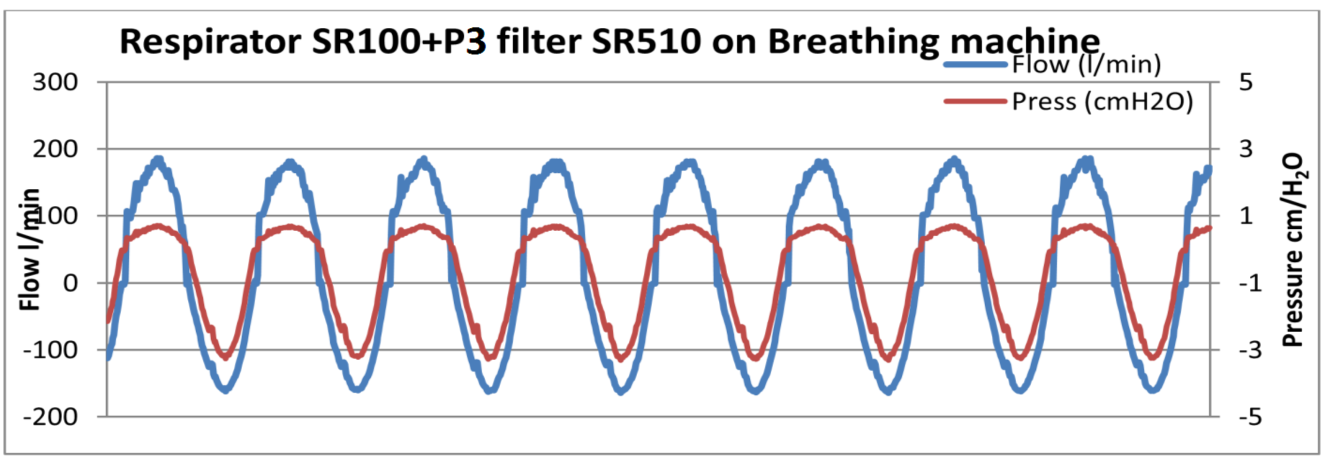

Figure 16: Pressure and flow inside the SR100 respirator with P100 filter on the breathing machine running 2 L tidal volume at 25 BPM.

The captured data combine the pressure inside the mask and the inhalation flow through the filter. Generally, the breathing machine profile is very close to sinusoidal (see Figure 16), so the peak flow for the volume of 2 L and 25 BPM breathing rate is expected to be π*2*25=157 L/min. The sum of all samples for the inhalation cycle is the lung volume and expected to be 2 L (breathing machine lung capacity).

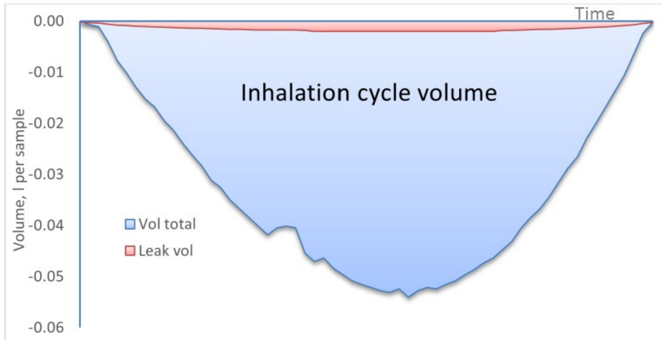

Figure 17: Inhalation Volume through the filter and through the orifice.

The calculation results from captured flow/pressure data inside the mask for the first inhalation cycle (see Figure 17) are as follows: The calculated Inhalation volume is 2.039 L. The maximum inhalation flow sample is 162.113 L/min. The results are very close to the expectation (2 L and 157 L/min), so we are satisfied with the achieved results.

Calculation of the Volume of Induced Leak

Because we know the flow/pressure characteristic of the orifices (see Face seal leak orifices and their characterization) and we know the pressure profile inside the mask for each inhalation breath, we can calculate the flow and then the volume of contaminated air getting into the mask through the orifice during inhalation cycles. The flow from the pressure across the orifice can be calculated with the following formula, which is derived from the equation that is shown below Figure 12 :

$$Vs = \frac{-b - \sqrt{b^2 - 4aP}}{2a * 3000}$$

where P = pressure cm H_2O; Vs = volume per sample; and a, b are coefficients which describe the orifice flow/pressure characteristic (see Figure 12). The value of 3000 converts the volume measured in 0.02 s to minute volume.

The total volume of the introduced leak for the inhalation cycle was the sum of the single leak volume Vs for all inhalation samples. In our case, the sample rate was 50 samples per second (20 ms per sample). The total leak volume for the inhalation cycle with a 2.8 mm orifice in diameter is calculated and plotted in red and equals 0.09287 L for this breath cycle (see Figure 17). The calculated protection level (%) was 1-0.09287/2.093=95.45%, very close to 95% for the 2.8 mm orifice (see Figure 14 and Table IV), which confirmed the validity of this method. Therefore, we can quantify the protection factor of the respirator with the size of the orifice (leak hole) which represents the imperfection in the mask seal. For example, for the given mask/respirator with nearly 100% efficient medium the imperfection of the face seal is equivalent to 2.8 mm hole in diameter (or equivalent of a leak cross-section of 6 mm^2); the protection level is reduced from 100% (see Figure 15) down to 95% of its theoretical value because of the leak only.

Comparison of the Ability of Different PAPRs to Compensate for Facepiece Leakage During Real Work

The assigned protection factor (APF) for a half-face negative-pressure respirator is 10 under the jurisdiction of OSHA and many other authorities. A PAPR conforming with AS/NZS 1716-2012 is a device designed to maintain positive pressure inside the facepiece by compensating for airflow during the inhalation cycle. The OSHA APF for a PAPR with full-face respirator is 1,000 (Occupational Safety and Health Administration, 2009), 100 times higher than for the negative-pressure respirator. It is also the user's expectation that the PAPR improves wearer comfort by reduction of breathing resistance: "*Because the motor blower pulls the air through the filter, breathing resistance virtually is eliminated.*" (Garvey, 2010-04-01). Our testing showed that in the real world, PAPR users may exhale against the motor's flow, and during inhalation, they may over-breathe the motor and therefore use their lungs to draw the air not only through the filter but also through the motor blower. Also, the PAPR is a dynamic system where the wearer randomly changes the intensity and the direction of the flow. Therefore, the user may assist the motor as it accelerates during inhalation, but when the exhalation cycle starts, the motor impeller should slow down. Because of the inertia, it is actually spinning at a higher speed, and it cannot slow down quickly enough. Users will breathe out at the same time as the impeller creates additional flow through the exhalation valve. This will increase the pressure in the mask during the exhalation cycle and adds additional exhalation breathing resistance instead of minimising it. During the opposite scenario, during the exhalation cycle, the motor decelerates and when the inhalation cycle starts, it is still running at a lower speed for some time. Now users will breathe through not only the filter but also through the slow running blower and the pneumatic arrangement.

There are many PAPRs which claim to be breath-responsive, i.e., to adjust motor speed according to the breathing to compensate for the air volume drawn by the user and to maintain the pressure inside the inner mask. It means that they are using additional power to accelerate the motor when pressure in the mask is reduced. This works well on slow breathing processes like the breathing machine during the tests, but on a real human with random breathing patterns, the positive pressure protection performance may even show a decline in performance compared to the PAPR with constant blower speed. In real life, the human breathing profile contains many high-frequency components, especially during speech segments, which the blower with variable speed cannot compensate, due to rotor inertia and the attached impeller inertia. So additional power, a noisier motor, heavier and high-power battery, as well as a high current motor control system, are required to accelerate and decelerate the rotor and the impeller. Therefore, the positive pressure dynamic performance of PAPR will be very much dependent on the design.

In this series of tests, we evaluated the performance of the PAPRs' positive-pressure leakage compensation. In addition, we compared different brands of PAPRs by simulating identical face seal leakage and calculated the concentration of contaminant that would leak into the respirator during the inhalation cycle. We used the same technique of introducing theoretical orifice leaks used for negative-pressure respirators as mentioned above. The series of tests was conducted on human subjects using a Monark bicycle ErgoMedic 839E with programming load capability and the pressure logger SE-RDA (Whitelaw, J., Jones, A., Davies, B. & Peoples, G., 2016). The test was performed using the same values each time (same bicycle profile, see Figure 18, same person once per day at the same time each day at 11am).

Figure 18: Monark bicycle ErgoMedic 839E (with SCBA + Full-face mask. Tested for reference).

Variation of air Consumption with Different Filter Resistance over the Same Work

Special attention was given to minimize the test-to-test variation, which includes the human subject. The variation between the tests and the effect of breathing resistance to volume consumption for the same exercise profile was evaluated. Our expectation was that the filter resistance variation would not make any significant difference to the minute ventilation and the total air consumption, as the Work of Breathing was very small compared to the work done during the exercise. To confirm this, we conducted a series of bicycle tests with 2 human subjects (Subj GP and Subj TS on Figure 20) using negative pressure respirator with 2 types of filters – a light P4 filter SR510 with small resistance and a combination of P4 SR510 and carbon ABE1 (SR315) filters with higher breathing resistance. The flow/pressure characteristics of these filters are shown in Figure 19. The test speech and bicycle load profiles are shown in Figure 21.

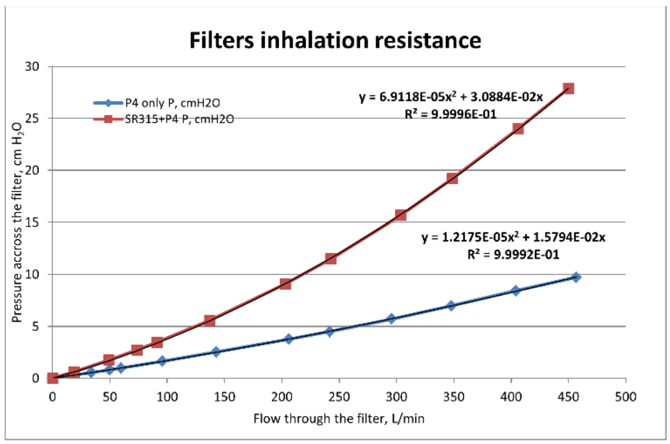

Figure 19: Low and high breathing resistance filters pressure-flow characteristics.

The air consumption for Subject GP and Subject TS over all exercises using the same profile is shown in Figure 20. The series of tests was repeated several times as follows:

- Subj GP: 5 tests are performed with P4 SR510 + SR315 filters: one of these tests is done 1 year prior to the rest of the tests
- Subj GP: 3 tests are performed with P4 filter only: one of these tests was done 1 year prior to the rest of the tests
- Subj TS: 3 tests are performed with P4 + SR315 filters
- Subj TS: 2 tests are performed with P4 filter only

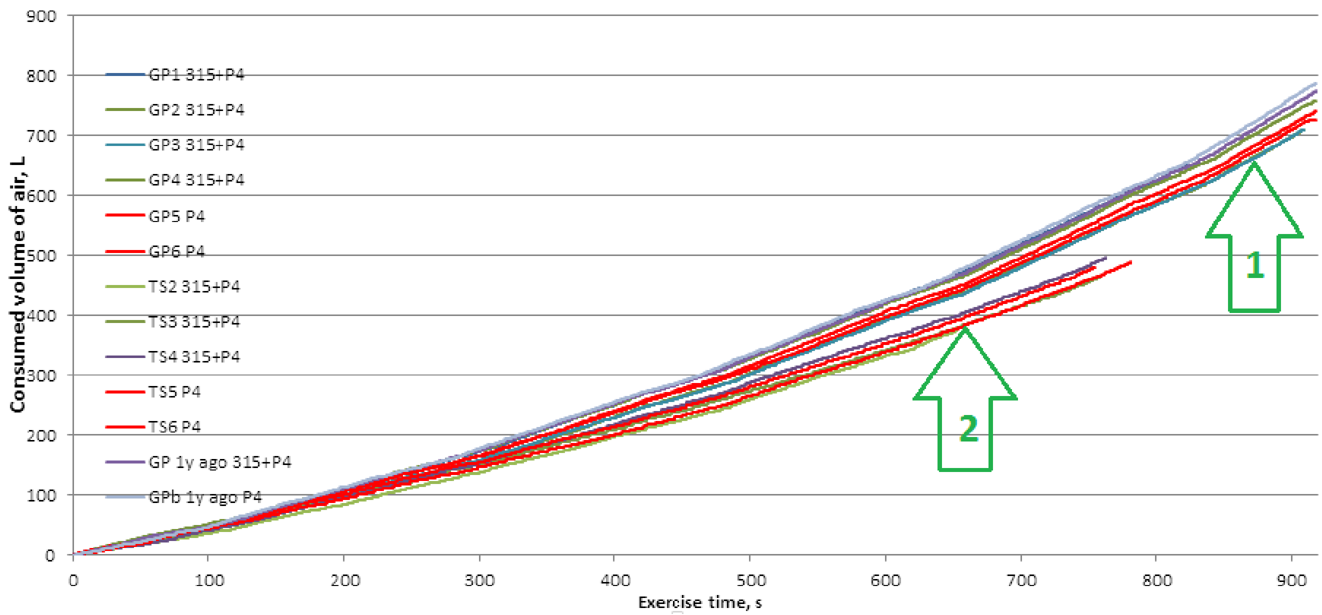

Figure 20: Air volume consumption for Subj 1 and Subj 2 at the same work profile for light resistance (red) and high resistance (dark) filters.

The consumed volume was measured by the SEA data logger SE-RDA (Whitelaw, J., Jones, A., Davies, B. & Peoples, G., 2016). It can be seen that the consumed air volume for low breathing resistance (particle filter SR510, red lined) and high breathing resistance (the combination of particle SR510 (P4) and carbon SR315 filters, dark lines) are the same.

We can see the variation in user air consumption is about 10% while the resistance for the SR510 and SR315 is about 2.5 times higher. The variation due to the filter resistance is masked by general data variation. Therefore, we can assume for our tests that the filter resistance affects the air consumption during the same work no more than the natural data variation in the tests. The total air consumption for Subject 1 for the period of 0-550 seconds exercise (light load) is 352 L and the total at 0-900 second (combination) is 702 L. This person was selected for the following PAPR tests.

Test Procedure

As presented in Figure 21 and Figure 22, the test method for each tested PAPR was as follows: the pressure in the mask for the same person riding the same bicycle with the profile shown on Figure 21 was monitored and recorded for different loads whilst reading periodically (red line on Figure 21) the standard “Rainbow” passage. The pressure inside the mask was continuously recorded for the entire duration of the exercise with the SE-RDA sample rate of 50 samples per second.

1. To simulate imperfections in the mask seal, the respirator’s pressure was converted to the leak flow during negative pressure events. Using this flow, the volume of contaminated air that entered the mask through the simulated mask leak was calculated.
2. With the assumption that the same person riding the same bicycle profile consumes approximately the same air volume during the same period of exercise, the PAPR protection level during the exercise could be calculated with an acceptable level of accuracy.
3. With the assumption that the same person riding the same bicycle profile consumes approximately the same air volume during the same period of exercise, the sum of the mask pressure variations (indicating the breathing resistance) over the same period can indicate the WoB for the PAPR (Eastern Illinois University) (Glenn Research Center, NASA). This value was compared with the

negative-pressure mask to see how the PAPR improves the breathing resistance for both the inhalation and exhalation cycles.

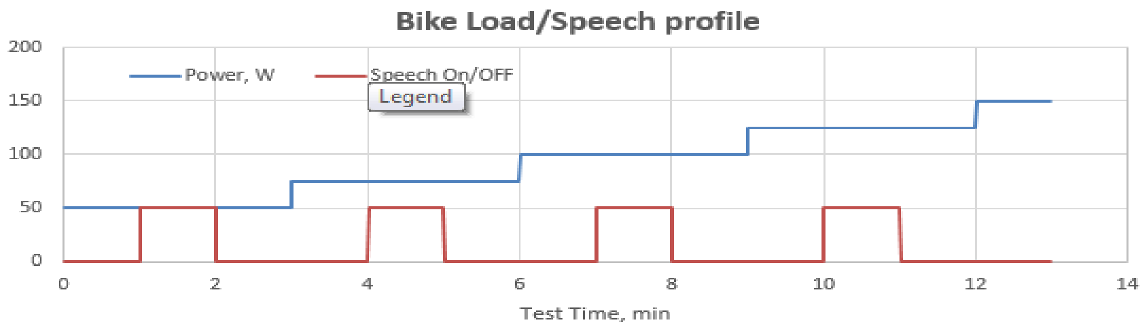

Figure 21: Test profile includes different load and speech pattern.

Figure 22: Test subject on the bicycle with different types of respirators.

To simulate the leak, we use the pressure/flow characteristics of a 2.8 mm orifice (equal to 95% reduction from our previous tests, see Figure 12).

Comparison of Different PAPRs' Ability to Compensate for Mask Leakage

For each tested PAPR, the graph shows the pressure inside the mask and the volume of contamination that entered the respirator during the inhalation cycles when the user over-breathes the unit, against time. The pressure variation for all graphs is presented at the same scale so we can visually compare the respirators' resistance. The contamination leak and pressure variation data are captured at 0-

550 seconds of the exercise (light load), 550 to 900 seconds (heavy load), and total at 0-900 seconds (combination) of the test for all units and shown with the green vertical marker on the top half of the graphs.

Firstly, an SCBA (Figure 23) and the negative pressure respirator (Figure 24) were investigated as two extremes in positive pressure performance. We can compare the positive pressure performance and breathing resistance of PAPRs with these reference devices.

SCBA+Full-face mask

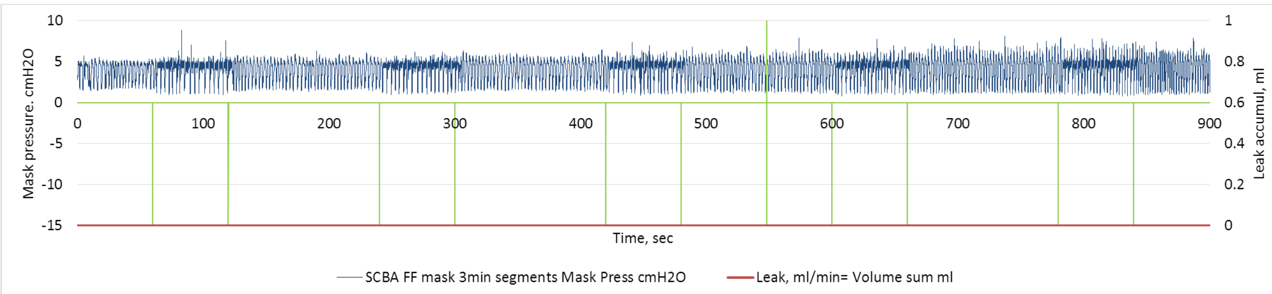

Figure 23 Spiromatic 90 SCBA+Full-face mask.

While the pressure variation of the SCBA is relatively high, the positive-pressure protection is excellent as no single negative-pressure event is recorded. We also can see the pressure variation inside the mask during inhalation and exhalation cycles is about 4 cm H_2O (varying from 1.5 to 5.5 cm for most breaths). Table V to Table XIII show the calculated inward leak and calculated respirator breathing resistance dP sum (the sum of delta pressure between each sampled measurements) for light part of exercise, heavy part and for total exercise. The speech portions are shown with the green vertical marker on the bottom half of the graphs.

Table V. Spiromatic 90 SCBA+Full-face Mask: Leak and Resistance

Parameters	Total	Light	Heavy
Leak Total, ml =	0.00	0.00	0.00
dP sum, cm H_2O =	7,744	4,181	3,562

Negative Pressure APR SR100 Half mask + P3 filters

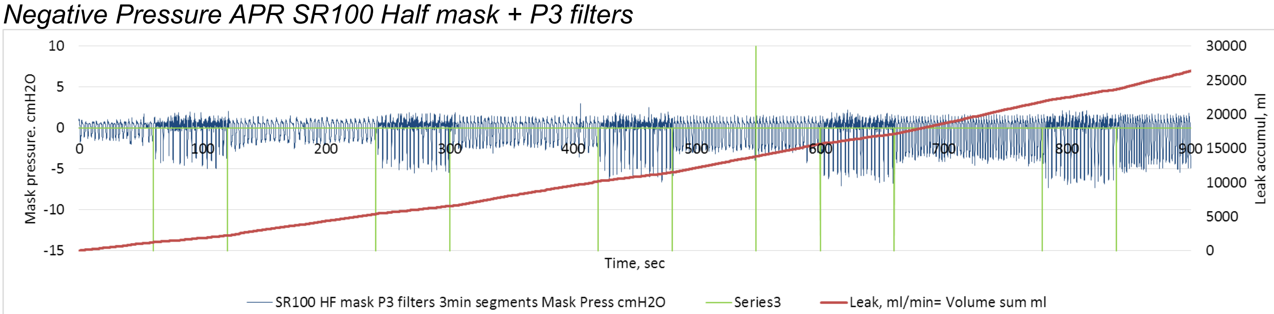

Figure 24 SR100 negative pressure Half mask + P3 filters.

The negative pressure SR100 shows small positive pressure excursions and larger negative pressure excursions, increasing with work rate. The SCBA (Figure 23) and the negative pressure mask (Figure 24) are added for comparison as units with the top positive pressure maintenance performance and which have no positive pressure performance (non-PAPR). These two graphs show that the breathing resistance during high workload is approximately the same, but during light workload the negative pressure respirator has less breathing resistance than the SCBA. At the same time during speech, the breathing resistance of the negative pressure respirator is higher than the one achieved with the SCBA.

Table VI. Negative Pressure Half mask + P3 filters: Leak and Resistance

Parameters	Total	Light	Heavy
Leak Total, ml =	26,307	13,823	12,484
dP sum, cm H_2O =	5,943	3,221	2,721

PAPR SE400 +P3 + Carbon SR315 filters + Full-face mask

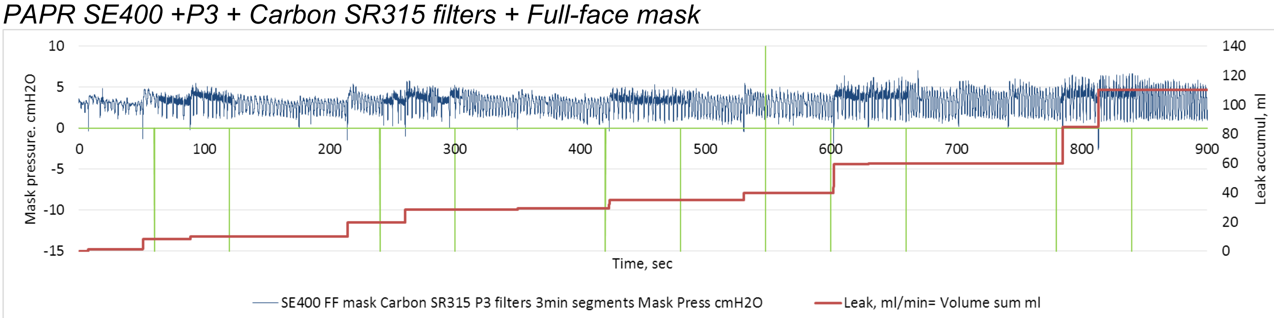

Figure 25 SE400 +P3 + Carbon SR315 filters + Full-face mask PAPR.

We can see some negative over-breathing events mostly during speech. The breathing resistance is slightly less that the negative pressure respirator (Figure 24) as the pressure variation is about 3 cm H_2O (from 1 to 4 cm). Here we can see the unique peculiarity of this machine as it accelerates close to negative pressure event: it very slowly decays the pressure while fast response is regulated by light demand valves. Here and in graphs below, please note the scale of the volume axis.

Table VII. SE400 +P3 + Carbon SR315 filters + Full-face mask PAPR: Leak and Resistance

Parameters	Total	Light	Heavy
Leak Total, ml =	110.2	39.7	70.5
dP sum, cm H_2O =	5,066	2,706	2,360

PAPR Shigematsu + P3 filters + Full-face mask

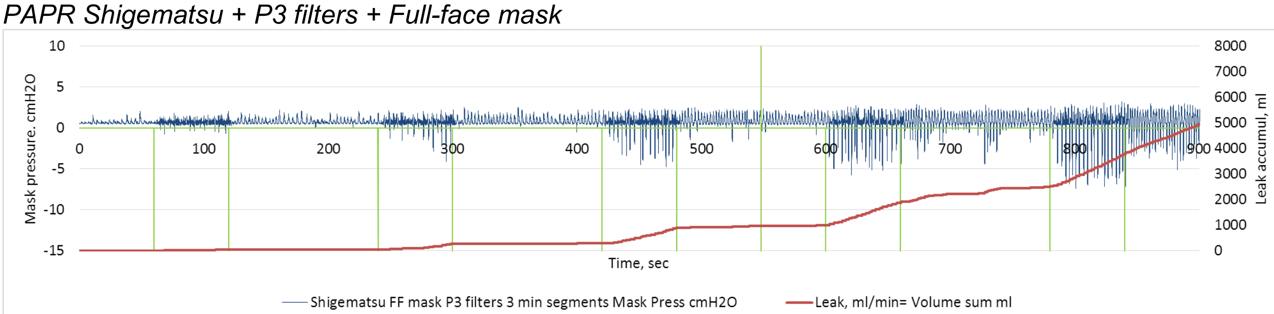

Figure 26 Shigematsu + P3 filters + Full-face mask breathe responsive PAPR.

This configuration is the breath-responsive unit with the small breathing resistance (see the general peak-to-peak pressure, and compare with graph for other units) and good performance on small workloads, whilst the pressure goes negative during the speech events.

Table VIII. Shigematsu + P3 filters + Full-face mask breath responsive PAPR: Leak and Resistance

Parameters	Total	Light	Heavy
Leak Total, ml =	4,927	956	3,971
dP sum, cm H_2O =	4,030	1,984	2,046

PAPR Paftec (CleanSpace) +P3+ Carbon filters + Half-face mask

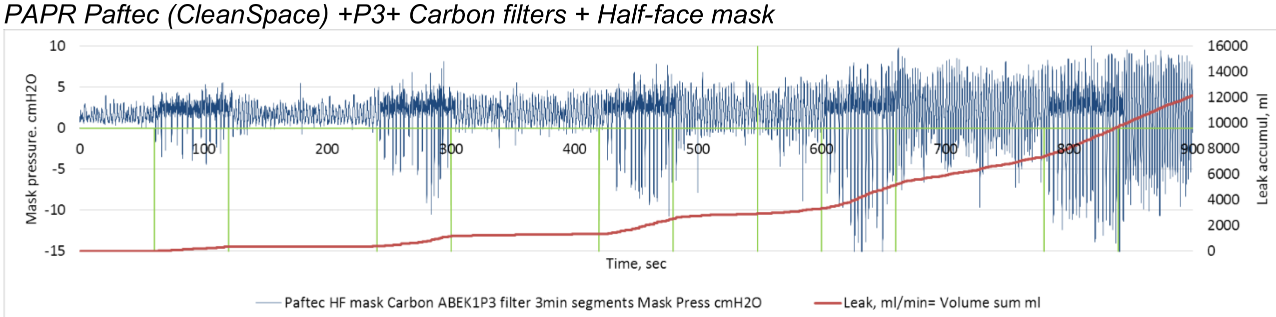

Figure 27 Paftec +P3+ Carbon filters + Half-face mask breathe responsive PAPR.

The breath-responsive unit struggles to keep up with speech and breathing especially during high workload events. This graph shows significantly higher breathing resistance than the negative pressure respirator (see Figure 24) because the pressure response to the breathing pattern is increasing significantly especially at high workloads.

Table IX Paftec + P3 + Carbon filters + Half-Face Mask Breathe Responsive PAPR: Leak and Resistance

Parameters	Total	Light	Heavy
Leak Total, ml =	12,114	2,913	9,202
dP sum, cm H_2O =	9,318	4,258	5,060

PAPR Sundström SR500 +P3+Carbon filter + Full-face mask

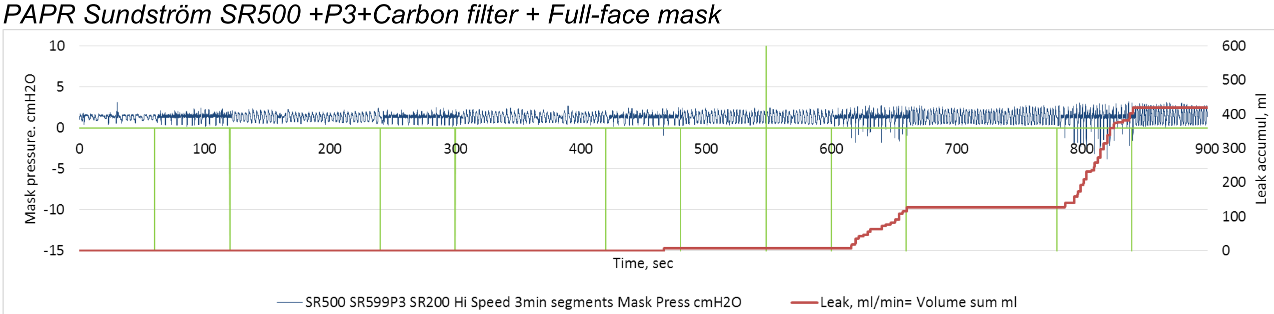

Figure 28 Sundström SR500 +P3+Carbon filter + Full-face mask PAPR.

This non-breath-responsive (constant flow) unit has excellent positive pressure performance at light and heavy workloads in the absence of speech but struggles to maintain the positive pressure inside the mask during speech events at high work. It has low breathing resistance across light and heavy workloads.

Table X. Sundström SR500 +P3+Carbon filter + Full-Face Mask PAPR: Leak and Resistance

Parameters	Total	Light	Heavy
Leak Total, ml =	420	6	414
dP sum, cm H_2O =	2,981	1,577	1,404

PAPR 3M VersaFlo TR302E + P3 + FF mask

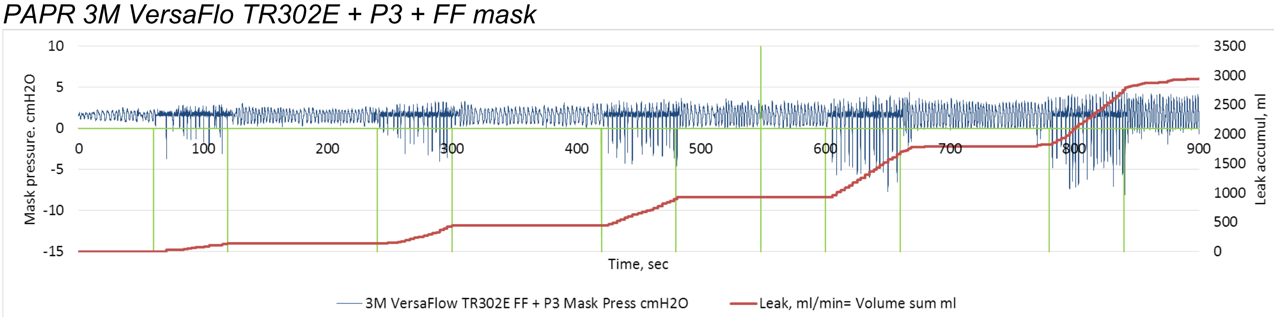

Figure 29 3M VersaFlo TR302E + P3 + FF mask PAPR.

This non-breath-responsive (constant flow) unit has very good negative-pressure performance at light and heavy workloads but struggles to maintain the positive pressure inside the mask during speech events. It has a small pressure response to the breathing pattern, which means it has a small breathing resistance especially at low workloads.

Table XI. VersaFlo TR302E + P3 + FF Mask PAPR: Leak and Resistance

Parameters	Total	Light	Heavy
Leak Total, ml =	2,936	925	2,011
dP sum, cm H_2O =	4,314	2,194	2,120

Negative Pressure Half-Face APR SR100 +P3+ Carbon SR315 filters

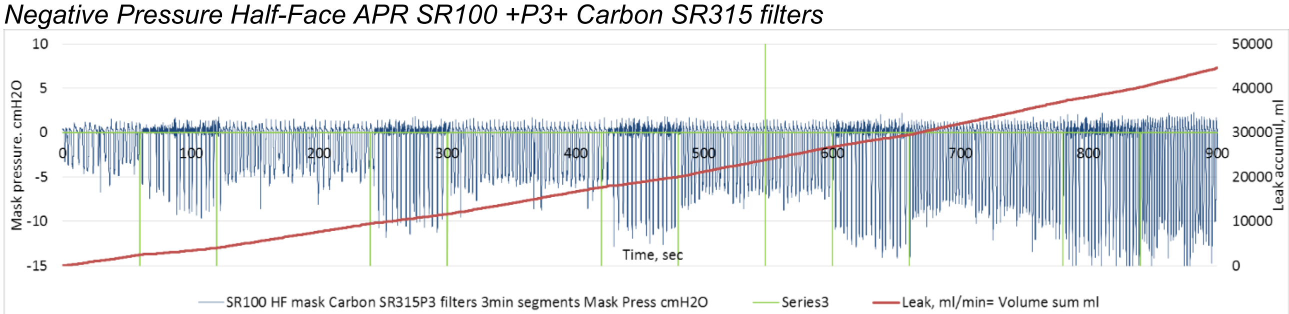

Figure 30 SR100 Half mask +P3+ Carbon SR315 filters (negative pressure).

For this negative pressure half-face respirator (same one as in Figure 24 but with an extra carbon filter providing higher inhalation resistance), we see a larger variation in pressure due to breathing and speech, as expected with a higher resistance, and a consequent larger leak rate.

Table VII. Negative Pressure SR100 Half Mask +P3+ Carbon SR315 filters: Leak and Resistance

Parameters	Total	Light	Heavy
Leak Total, ml =	44,502	23,789	20,714
dP sum, cm H_2O =	8,648	4,226	4,422

Negative-pressure Full Face APR SR200 with P3 and carbon filter SR315

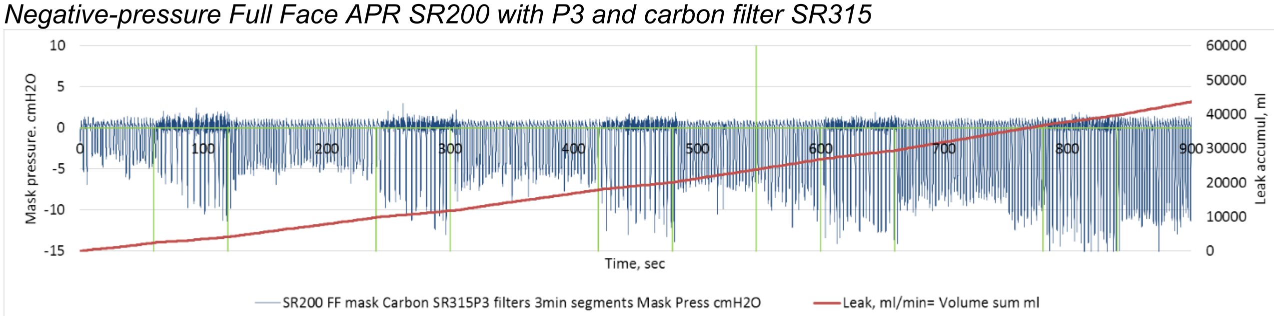

Figure 31 Negative-pressure respirator full-face SR200 with P3 and carbon filter SR315.

Results for the negative pressure full-face respirator are added for comparison with the half-face respirator. We see no significant difference between the two in terms of air path protection and breathing resistance.

Table XIII. Negative-Pressure Full-Face Respirator SR200 with P3 and Carbon Filter SR315: Leak and Resistance

Parameters	Total	Light	Heavy
Leak Total, ml =	43,650	23,887	19,764
dP sum, cm H_2O =	10,219	5,600	4,619

Summary

The Protection factor and Work of Breathing for different PAPRs having a leak equivalent to a 2.8 mm hole are shown in Table V. The blue row highlights the test with the carbon filter, the green and yellow the negative pressure respirators shown as the references, and green shows the tests with the gas filters. The columns "ratio to NPR" shows the values referenced to APR SR100 HF mask with P3 filter.

Table XIV. Protection Factor and Breathing Resistance for Different PAPR having a Mask Leak the equivalent of 2.8mm hole

Device Under test	Consumed Contaminated air, mL	Protection, ratio to NPR	Protection with leak 2.8 mm diam	dP (~WoB) dP sum, cm H2O	dP (~WoB) dP sum, ratio to NPR
Breath responsive SCBA Spiromatic 90 FF mask	0	∞	70,000	7,744	1.30
Breath responsive PAPR SE400 HF mask P3 filters	13.73	1,916.34	50992	5992	1.01
Breath responsive PAPR SE400 FF mask P3 filters	41.98	626.63	16,674	4,927	0.83
Breath responsive PAPR SE400 FF mask Carbon SR315 P3 filters	110.19	238.75	6353	5066	0.85
Constant flow PAPR SR500 P3 SR200 Hi Speed	232.08	113.35	3,016	2,877	0.48
Constant flow PAPR SR500 SR599P3 SR200 Hi Speed	419.95	62.64	1,667	2,981	0.50
Constant flow PAPR SR700 PAPR SR200 FFM P3 single hose	638.73	41.19	1,096	2,821	0.47
Constant flow PAPR SR500 P3 SR900 HFM twin hose	703.66	37.39	995	2,865	0.48
Constant flow PAPR 3M VersaFlo TR302E FF + P3	2,936.17	8.96	238	4,314	0.73
Breath responsive PAPR Shigematsu FF mask P3 filters	4,927.03	5.34	142	4,030	0.68
Breath responsive PAPR Paftec HF mask P3 filters	8,438.67	3.12	83	7,935	1.34
Breath responsive PAPR Paftec FF mask P3 filter	8,743.39	3.01	80	6,711	1.13
Breath responsive PAPR Paftec HF mask Carbon ABEK1P3 filter	12,114.89	2.17	58	9,318	1.57
APR SR100 HF mask P3 filters	26,307.09	1.00	27	5,943	1.00
APR SR200 FF mask P3 filters	31,213.26	0.84	22	7,145	1.20
APR SR200 FF mask Carbon SR315 P3 filters	43,650.35	0.60	16	10,219	1.72
APR SR100 HF mask Carbon SR315 P3 filters	44,502.35	0.59	16	8,648	1.46

Note: NP – Negative Pressure, FF – Full-face, HF – Half-face, FFM – Full-face Mask, HFM – Half-face Mask, NPR – Negative Pressure Respirator

We can see that the pressure variation caused by inhalations and exhalations, representative of the breathing resistance of a respirator, does not show as much variation as the differences in the respirator protection. Furthermore, some PAPRs have even larger pressure variation in comparison to the negative-pressure respirator (SR100 respirator results were shown in this table as the reference). However, we can see that the main difference in PAPRs is the leak compensation, which depends on the PAPR design. For example, with the same respirator leak, the inward leakage of Paftec HF mask with P3 filter was about 2.17 times less than with the NPR while the SE400 HF mask with P3 filter provides more than 1,900 times reduction in the inward leakage of the face with the same sealed conditions. At the same time, while the breathing resistance with the Paftec unit was 1.13 times higher than the negative-pressure respirator, with the SE400 the breathing resistance was almost the same as the NPR. Therefore, according to these results, some PAPRs are more efficient for mask seal leak compensation than others, and this performance varies significantly. The breathing resistance also varies significantly, becomes smaller, and, as we can see, for some PAPRs is not necessarily less than the resistance of negative pressure respirators. Therefore, we can conclude that the PAPRs are not as much breathing-assisting respirators as they are mask-leak compensation devices. The PAPR provides additional face seal protection to the wearer in the event of mask leakage.

Currently there is no direct test that evaluates the efficiency of the positive-pressure compensation of a PAPR. The existing tests are based on constant flow, or, in the best-case scenario, based on a slow sinusoidal breathing machine profile. As discussed above, the PAPR shows a deterioration in efficiency on humans during real work compared to the artificial test on a sinusoidal breathing machine or based on constant flow because of random breathing patterns of humans, which present significant energy of high-frequency components in the pressure spectrum. Therefore, breath-responsive PAPRs may not react fast enough to the fast pressure changes inside the mask. The respirator wearer can breathe in-phase with the motor and the next moment the blower can work out of phase with the user, which increases the breathing resistance.

The existing TIL test with human subjects evaluates the combination of the mask seal and the PAPR performance. A fit test before the TIL test with the power off is prescribed to ensure the correct mask size is chosen, but does not reflect performance in positive pressure mode. The TIL test combined with pressure measurement is needed to demonstrate performance in use and whether the blower unit is able to adequately compensate for breathing and speech particularly at higher work rates. Otherwise, problems with positive-pressure performance may remain unnoticed and vice versa, if the PAPR performance is sufficiently high, it can be difficult to accurately quantify the face fit.

These experiments demonstrate that the Work of Breathing for some PAPRs can be even greater than that of some negative-pressure respirators. PAPRs' ability to maintain positive pressure cannot be assessed by constant-flow measurement or by the sinusoidal profile of a breathing machine, but it can be assessed by collecting the pressure inside the mask during TIL human exercise in parallel with the TIL test and analysing the "weight" of the negative-pressure events.

The study shows that while the flow rate claimed for PAPRs by manufacturers varies by 2-3 times, the actual level of protection provided by the positive pressure varies by hundreds of times, while the ability of PAPR to track the breathing pattern inside the mask and keep the pressure constant during inhalation and exhalation varies significantly between different PAPR models. Therefore, the ability to maintain positive pressure is the major factor that characterizes the protection factor of different PAPRs, while the "Work of Breathing" varied less between PAPRs. Acknowledging this and testing positive-pressure performance during the certification would encourage manufacturers to invest in new technology, which may improve the protection performance of PAPRs.

References

Australian/New Zealand Standard AS/NZS, 1716:2012. (n.d.). *Respiratory Protective devices, 1716:2012.*
Dr Billy Markus Drew. (n.d.). Oxygen Consumption and Delivery. Summary.

Eastern Illinois University. (n.d.). Work Done by Gas. *http://ux1.eiu.edu/~cfadd/1150/14Thermo/work.html*.

Ian Stewart Laird. (1995). The Physiological Costs of Wearing Respiratory Protective Devices. *Massey University*.

Garvey, D. J. (2010-04-01). Constructing a Powered Air Purifying Respirator System. *https://www.ehstoday.com/ppe/respirators/article/21906717/constructing-a-powered-air-purifying-respirator-system*.

Glenn Research Center, NASA. (n.d.). Work Done by Gas. *https://www.grc.nasa.gov/WWW/K-12/airplane/work2.html*.

ISO/TS 16976-4:2019, Respiratory protective devices. (n.d.). *Respiratory protective devices — Human factors.*

Occupational Safety and Health Administration. (2009). Assigned Protection Factor for the Revised Respiratory Protection Standard.

Scott J Butcher, R. L. (n.d.). Work of breathing is increased during exercise with the self-contained breathing apparatus regulator. *https://pubmed.ncbi.nlm.nih.gov/17213883/*.

Whitelaw, J., Jones, A., Davies, B. & Peoples, G. (2016). *Evaluation of a Personal Data Logger to Measure Real-Time Breathing Cycles Across Varying Work Rates.* The 18th International Conference of International Society for Respiratory Protection.